Available online at www.CivileJournal.org

# Civil Engineering Journal

(E-ISSN: 2476-3055; ISSN: 2676-6957)

Vol. 9, No. 05, May, 2023


# Fire Resistance Analysis of Two-Way Reinforced Concrete Slabs

Fidan Salihu [1], Zijadin Guri [1*], Meri Cvetkovska [2], Fatos Pllana [1]

[1] *Faculty of Civil Engineering, University of Pristina "Hasan Prishtina", Pristina 10000, Kosovo.*

[2] *Faculty of Civil Engineering, University "Ss. Cyril and Methodius", Skopje 1000, North Macedonia.*

Received 06 February 2023; Revised 17 April 2023; Accepted 24 April 2023; Published 01 May 2023

**Abstract**

This paper presents a fire resistance analysis of two-way reinforced concrete (RC) slabs. The study analyzes the effect of specific parameters—concrete cover thickness, span, and support conditions—on the fire resistance of the slabs. To that end, the slabs were exposed to Standard Fire ISO 834, and the 3D nonlinear numerical analyses were conducted in SAFIR2016. The results of the numerical analyses were evaluated against experimental results reported in the literature. The agreement between the two sets of results was satisfactory throughout the fire test. Nonetheless, to verify the obtained numerical results, all testing-related parameters must comply with the numerical simulation results. This comparison demonstrated the usefulness of numerical simulations in predicting the behavior of structures in fire conditions. In addition to the nonlinear numerical analysis, the fire resistance was calculated using the simplified method and tabulated data described in Eurocode 2 (Part 1.2) to assess the accuracy and reliability of fire safety regulations in the design of two-way slabs and identify significant differences between the design code and numerical analysis. The comparison showed that SAFIR2016 provides more accurate results by considering additional factors, such as tensile membrane forces, which increase the fire resistance of two-way slabs. According to the load-bearing criteria, the two-way slabs have high fire resistance, considerably higher than prescribed in the fire safety regulations, which ignore the positive effect of tensile membrane forces. According to the numerical analysis, the upper reinforcement in the compression areas of the slab's span was considered, which increased the fire resistance of the slabs. In contrast, according to the design codes, the contribution of this reinforcement is neglected. It was indicated that the increased concrete cover improves the fire resistance of the slabs. The vertical displacements increase by increasing the slab span, but according to the load-bearing criteria, all the slabs show fire resistance of over ten hours. In terms of bearing capacity, slabs with various support conditions show fire resistance of longer than ten hours. In terms of deflections, the supporting conditions of the slabs have a significant influence on their behavior. This study provides valuable insights into the fire resistance of two-way RC slabs and highlights the importance of considering specific parameters in the analysis.

*Keywords:* Two-Way RC Slabs; Fire Resistance; 3D Analysis; SAFIR2016.

## 1. Introduction

In the event of a fire, floor slabs play a crucial role in separating fire compartments and preventing the spread of fire and smoke. As such, these slabs must be treated to withstand the prescribed time of fire exposure and maintain their integrity and insulation criteria [1]. The treatment should also limit thermal radiation on the unexposed side. Analyzing the behavior of reinforced concrete slabs under fire conditions is of paramount importance in ensuring the safety of occupants during a fire since reinforced concrete is commonly used in construction operations.

The literature on the fire behavior of reinforced concrete slabs has extensively expanded over the years. The full-scale fire tests carried out at Cardington showed that the membrane tension forces in the composite slabs have a key

* Corresponding author: zijadin.guri@uni-pr.edu

http://dx.doi.org/10.28991/CEJ-2023-09-05-05

© 2023 by the authors. Licensee C.E.J, Tehran, Iran. This article is an open access article distributed under the terms and conditions of the Creative Commons Attribution (CC-BY) license (http://creativecommons.org/licenses/by/4.0/).

influence on the increase in fire resistance [2]. Lim & Wade [3] studied fire-exposed floor slabs by mainly focusing on the influence of compressive membrane action in one-way slabs and tensile membrane action in two-way concrete slabs. It was found that two-way simply supported slabs have much greater fire resistance than one-way simply supported slabs. It was also reported that the high fire resistance of two-way slabs is due to tensile membrane action. Bailey and Toh [4] tested the concrete slabs at ambient and elevated temperatures. Two modes of failure were observed at ambient temperature, comprising fracture of the reinforcement or crushing of the concrete at the corners of the slab. At elevated temperatures, all the tests failed due to a fracture of the reinforcement. The reinforcement lost greater strength compared to the concrete in the corners of the slab, where crushing was observed in the ambient tests and led the reinforcement fracture to be the critical failure mode. Jiang & Li [5] numerically investigated the mechanism of the tensile membrane action developed in reinforced concrete slabs at large displacements and elevated temperatures. In that study, five failure modes of slabs initiated by the rupture of reinforcement were found depending on the boundary condition, reinforcement layout, and aspect ratio. It was suggested to increase the reinforcement ratio to enhance the effect of tensile membrane action.

Wang et al. [6] proposed a transient strain model of concrete with a transient modulus under the biaxial stress state and a failure criterion to determine the fire resistance of two-way reinforced concrete slabs. The transient strain introduced into the concrete constitutive model enables the program to predict slab deflection and fire resistance values accurately. The creep strain of steel bars considerably affects the deflection of a slab at high temperatures. Hence, the numerical simulation should include this strain. It was found that the thermal strains of concrete and steel, particularly that of concrete, have a considerable effect on slab deflection and fire resistance at elevated temperatures. Greater thermal strains in concrete could lead to greater deflection and smaller fire resistance in the slab. Therefore, the fire resistance of the slab could be conservatively estimated using the thermal strain models of concrete and steel from Eurocode 2. Liao & Huang [7] developed a model with an excellent numerical technique to assess the structural stability (global behavior) and integrity (localized fracture) of reinforced concrete members in the fire. The proposed model can be applied to modeling localized fracture of reinforced concrete slabs under fire conditions to assess the integrity failure of concrete floor slabs.

Many simplified methods have been developed to determine the ultimate load capacity of slabs exposed to fire. Many of which use the theory of the behavior of slabs at ambient temperature at large displacements for the case of exposure to high temperatures, considering only the reduction of the strength and stiffness characteristics of concrete and steel at high temperatures while ignoring the effects of thermal expansion and thermally induced buckling. Depending on the proposed methods, there is a substantial difference in the behavior and shape of the fracture of the slabs and the real behavior at ambient temperature and high temperatures when exposed to membrane tension forces. Abu et al. [8] proposed a new analytical method to determine the behavior of slabs exposed to fire that includes thermal and mechanical effects. For this purpose, they used the Rayleigh-Ritz variational approach from the classical slab theory at large displacements. This method improves the accuracy of determining displacements and membrane tension forces. Nonetheless, stress determination requires more accuracy. In that study, the results were compared with numerical modeling results using Vulcan.

It has been demonstrated that in a fire, floor slab failure is typically characterized by significant displacements. If the slab is close to its limit state, residual deformations can be extended after the cooling phase, necessitating repairs. Therefore, the deformation or deflection of the slab must be limited to the prescribed value [2-4]. According to the ISO standard, the limit value for deflection is L/30, where L is the span of the slab [9]. This ensures that the slab remains within the safe limits of deformation during a fire incident and can be repaired afterward if necessary.

These studies provide valuable insights into the behavior of reinforced concrete slabs in the event of a fire. Nonetheless, the influence of specific parameters on the fire resistance of two-way RC slabs needs further research to understand their behavior under fire conditions and to develop more effective fire protection strategies. In our research, several parameters that have been ignored in previous research were addressed to draw a more realistic picture of the behavior of reinforced concrete slabs in fire incidents. Furthermore, numerical 3D analyses were conducted using SAFIR2016 to determine the extent to which different parameters—concrete cover thickness, slab span, and support conditions—affect the fire resistance of two-way reinforced concrete slabs. In addition, the results obtained from the numerical analysis were compared with those obtained through the methods given in the design code [1]. Bearing in mind that the design codes of the relevant countries are used for the design of construction engineering structures from the impact of fire, through this work, we will give recommendations on the design of two-way reinforced concrete slabs according to the methods given in Eurocode [1]. At what level of safety is it, how much is conservative, and can they be optimized?

Here, single-span slabs exposed to fire from the bottom side and subjected to standard fire ISO 834 until failure were analyzed. To compare the results, the fire resistance was also calculated using the Yield Line Theory for slabs [10], which takes into account the reduced tensile strength of steel at high temperatures. The temperatures in the reinforcement were obtained using SAFIR2016 [11], while the strength and deformation properties of the reinforcing steel at elevated temperatures were adopted according to the reduction coefficients provided in EN1992-1-2 [1]. In this analysis, it was assumed that the surface of the reinforcement is equal to the required reinforcement according to EN1992-1-1 [12].

Overall, these analyses provide valuable insights into the extent to which the mentioned parameters impact the fire resistance of two-way reinforced concrete slabs and can help develop more effective fire protection strategies for these structures.

## 2. Research Methodology

First, the existing literature was reviewed to identify and organize key findings, procedures, and limitations. In the next step, the results of the numerical analyses were compared with experimental results reported in the literature. The two sets of results throughout the fire test agreed sufficiently. Then, a parametric analysis was performed on the fire resistance of two-way reinforced concrete slabs. The effects of concrete cover thickness, slab span, and support conditions on the fire resistance of two-way reinforced concrete slabs were analyzed using the methods given in EN1992-1-2 [1] and numerical 3D analysis in SAFIR2016. The obtained results were then analyzed, and the fire resistance of two-way slabs was compared according to SAFIR2016 results, a simplified method, and tabulated data given in EN1992-1-2 [1]. Finally, the research conclusions were summarized. The research methodology flowchart is shown in Figure 1.

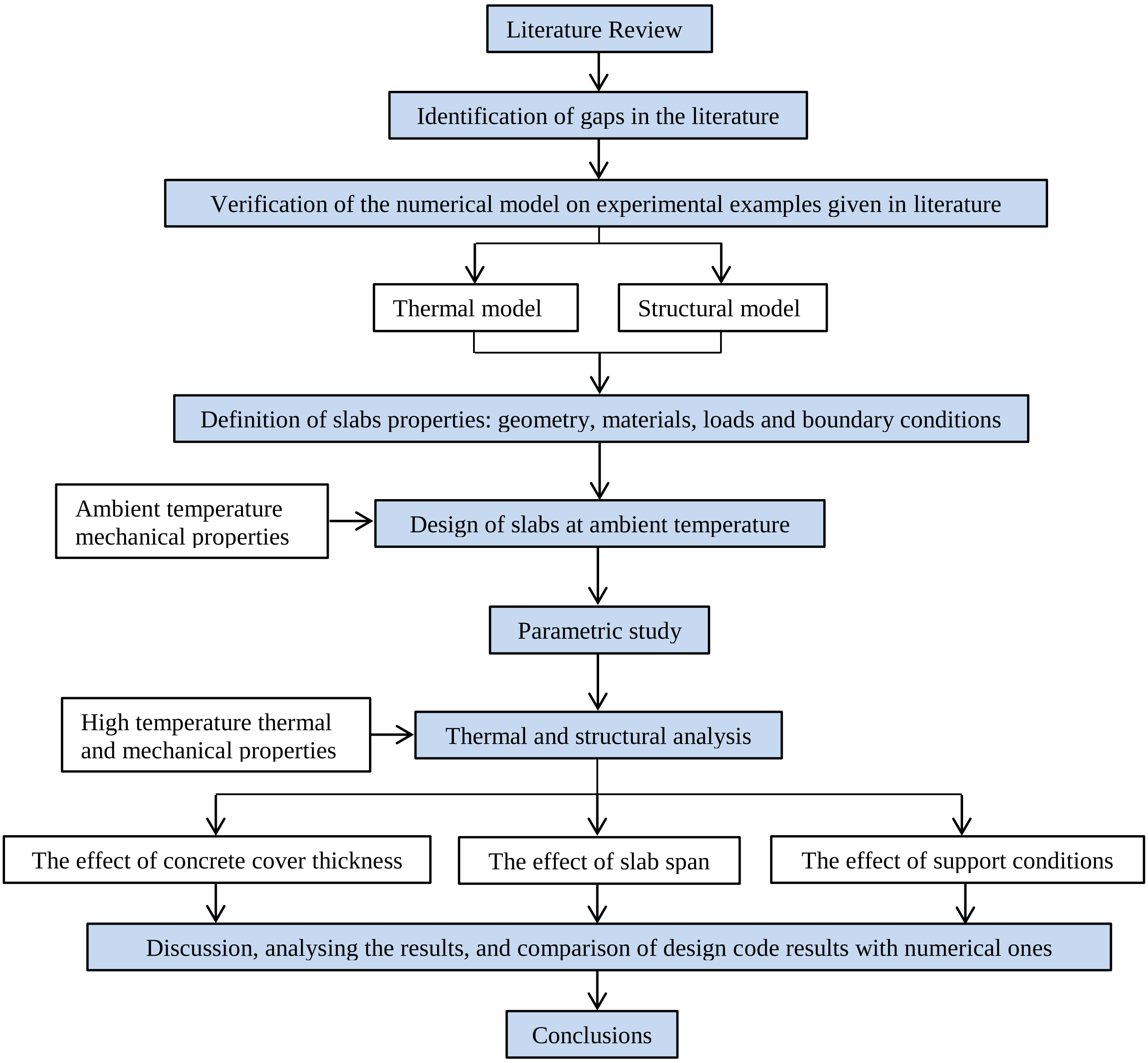


**Figure 1. The considered methodology**

## 3. Numerical Model

The analysis was conducted using the finite element software SAFIR2016. The constitutive material models for concrete and steel were used according to EN1992-1-2 [1], while the thermal action was defined using a standard ISO 834 fire curve. The analysis procedure required the development of two separate models with the same geometry: a thermal model and a structural model. The thermal model was used to analyze the transient thermal response of the structure under the specified thermal loads. It takes into account the material properties and the heat transfer characteristics of the structure and calculates the temperature distribution and thermal gradients within the structure. The structural model was used to analyze the transient mechanical response of the structure under combined thermal and mechanical loads. It considers the thermal loads obtained from the thermal model and calculates the deformation, stresses, and strains within the structure.

### 3.1. Thermal Model

To perform a structural analysis of the slabs at each time interval, the output data from the thermal analysis of the fired elements should be employed. The finite element mesh used in the structural analysis should be compatible with the mesh used in the thermal analysis, hence the need for a 3D analysis. The temperature distribution and resulting thermal stresses can vary significantly across the thickness of the slab.

Figure 2 shows a cross-sectional discretization of a slab for 3D thermal analysis. The thickness of the slabs is specified as 16 cm, and they have been discretized using 32 rectangular elements with four nodal points. This type of discretization ensures the accuracy of calculating temperature distributions throughout the thickness of the slab.

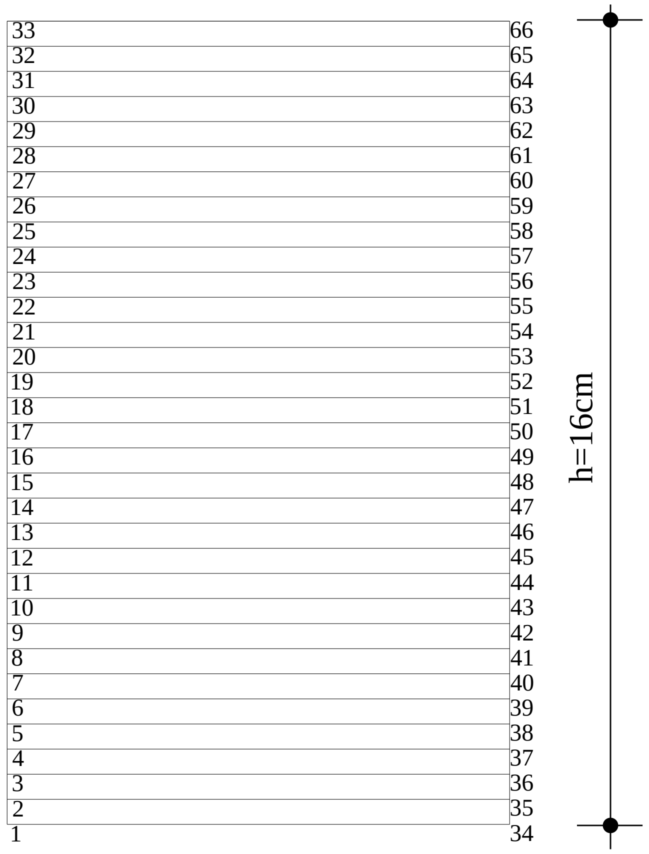


**Figure 2. Discretization of a slab cross-section for 3D thermal analysis**

In thermal analysis, heat transfer in the plane section is by conduction, and the coefficient of thermal conductivity is taken according to the lower curve given in EN1992-1-2 [1]. Convection coefficients $\alpha_c$=25 Wm$^{-2}$°C$^{-1}$ and $\alpha_c$=9 Wm$^{-2}$°C$^{-1}$ are adopted for exposed and unexposed surfaces, respectively, while emissivity related to concrete surface is adopted as $\varepsilon_m$=0.7, according to EN1992-1-2 [1].

### 3.2. Structural Model

The symmetry of the slabs was used in the analysis. Figure 3 shows a 3D model of a simply supported slab using symmetry. This model represents only one-quarter of the slab, with the other three-quarters being identical due to the symmetry of the problem. This model could improve the efficiency of the analysis while providing accurate results for the behavior of the entire slab. Overall, the use of symmetry in the analysis of two-way reinforced concrete slabs is a common technique to simplify the computational process and reduce the resources required while still providing accurate results.

After the model was defined, the specified load and thermal conditions were applied to the slab, and the equations of equilibrium and compatibility using were solved via finite element analysis. The results of the analysis provided information on the behavior of the slab, including its stress and strain distribution, deflection, and failure modes, under the specified load and thermal conditions. This information can be used to optimize the design of the slab and develop more effective fire protection strategies.

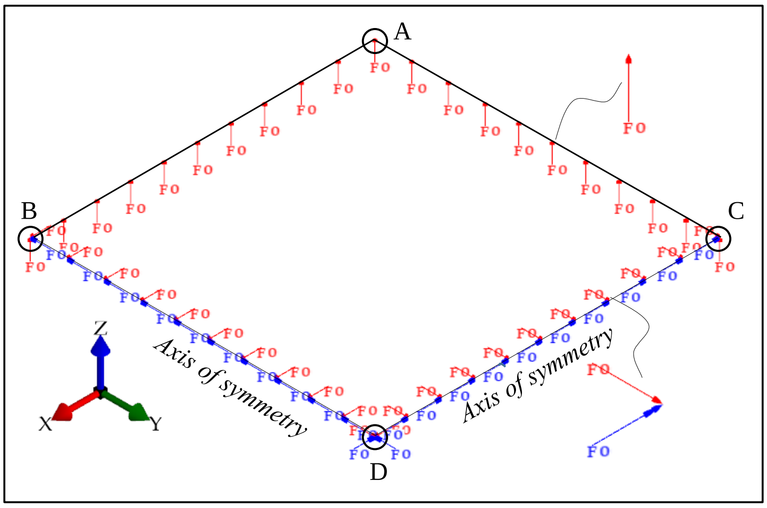


**Figure 3. The 3D model of a simply supported slab for structural analysis in SAFIR2016**

The reinforced concrete slab in SAFIR2016 is discretized using rectangular shell elements with local axes parallel to the global axes (Figure 4). These elements are well-suited for modeling thin, two-dimensional structures such as slabs. During the analysis, the rectangular shell elements were subjected to the specified loads and thermal conditions, and the resulting stresses and strains were calculated. The stresses and strains were then used to determine the deformation and failure of the slab under these conditions. Overall, the use of rectangular shell elements with local axes parallel to the global axes is a common approach in SAFIR2016 for discretizing and analysing reinforced concrete slabs. This method improves the efficiency and accuracy of the analysis of these structures under various load and thermal conditions.

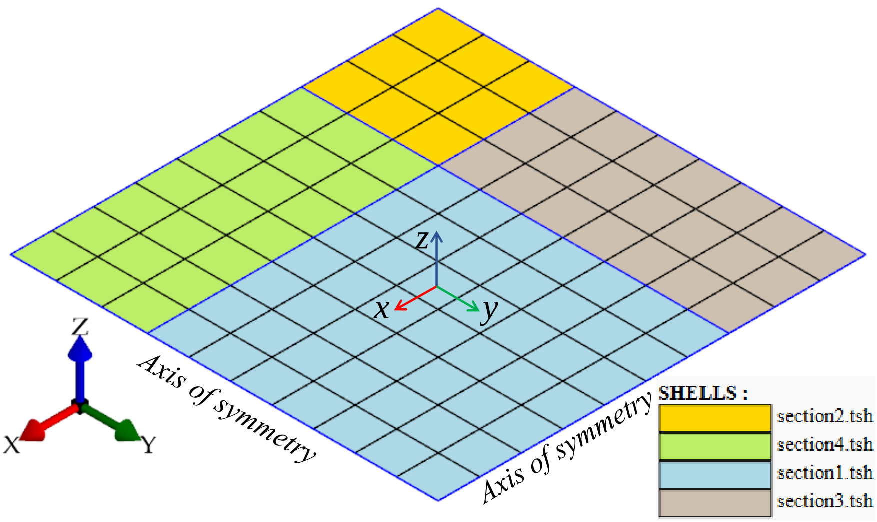


**Figure 4. Reinforced concrete slab discretized with rectangular shell elements with local axes parallel to the global axes**

# 4. Verification

## 4.1. Verification of the Software SAFIR2016 for Thermal Analysis of Fire-Exposed Slabs

Figure 5 compares the temperature distribution for a 200 mm thick slab obtained with SAFIR2016 and the isotherms in EN1992-1-2 [1]. The diagrams show that the temperature distribution in the cross-section of the slab agrees with the isotherms provided in EN1992-1-2 [1]. This indicates that SAFIR2016 incorporates the recommendations given in the latest version of EN1992-1-2 [1].

The temperatures used in the analysis were calculated for a slab made of concrete with silicate aggregate, and the coefficient of thermal conductivity is taken according to the lower curve given in EN1992-1-2 [1]. The coefficient of emission is adopted at *0.7*, which is a typical value for concrete.

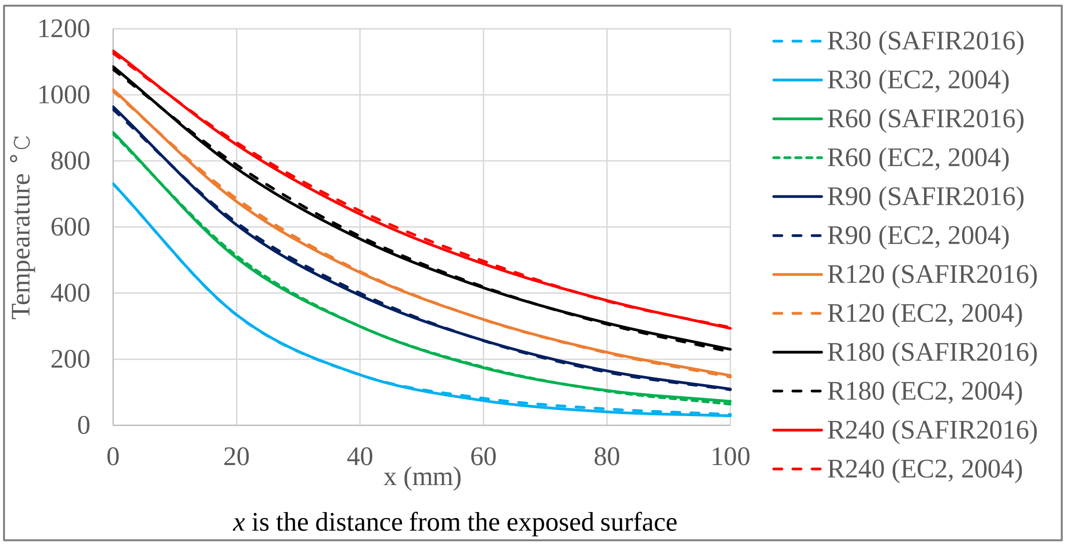


**Figure 5. Comparison of temperatures in a slab with a thickness of 200 mm, obtained with SAFIR2016 and the recommendations given in Eurocode 2, part 1-2 [1]**

Figure 6 displays the temperature distribution in the cross-section of a 100 mm thick slab over time. The temperatures numerically calculated were compared to experimentally obtained temperatures during a fire test of the slab [3]. The temperature rise over time is demonstrated for three surfaces: the exposed side (*x=0 mm*), the middle of the slab (*x=50 mm*), and the unexposed side (*x=100 mm*). For the exposed side, the SAFIR2016 version estimates higher temperatures than the experimentally obtained values. However, the calculated temperatures show similar trends over time, which could be attributed to the unknown physical and mechanical properties and temperature dependence of materials.

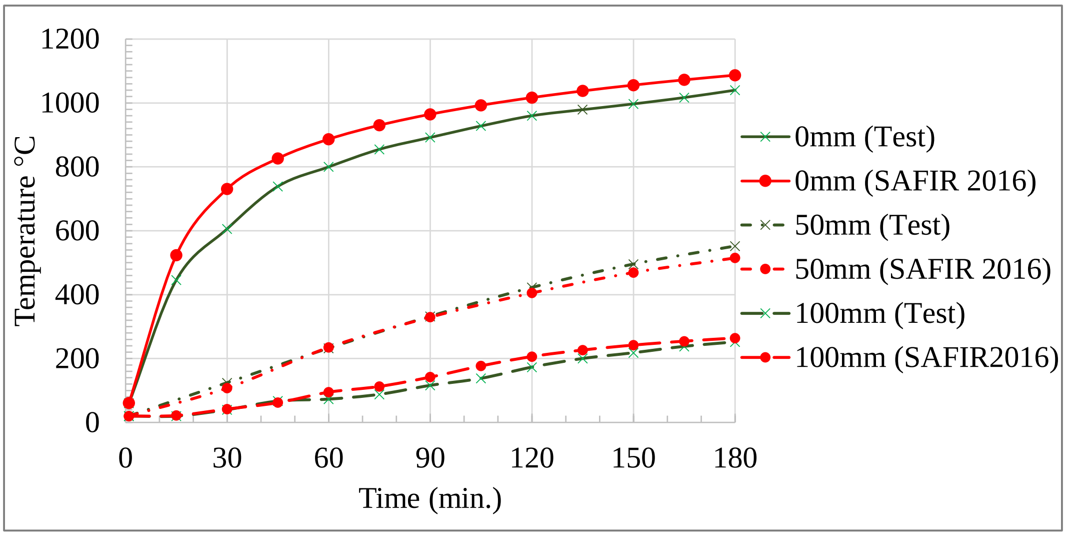


**Figure 6. Comparison of temperatures calculated with SAFIR2016 with the experimentally obtained temperatures for a 100 mm thick slab exposed to ISO fire**

The overall comparison results between numerical and experimental temperature data suggests that SAFIR2016 can accurately predict the temperature distribution in reinforced concrete slabs under fire conditions. This further validates the use of SAFIR2016 for analysing the fire resistance of reinforced concrete slabs.

### 4.2. Verification of the Software SAFIR2016 for Structural Analysis of RC Slabs Exposed to Fire

Table 1 specifies the properties of the tested flat slabs exposed to the ISO fire [3]. The comparison between numerical and experimental results is a crucial step in verifying the accuracy and reliability of any simulation software. The good agreement between the numerical simulations performed using SAFIR2016 and the experimental results obtained by Lim and Wade [3] (Figure 7) ensures that the software can optimally predict the behavior of reinforced concrete slabs under fire conditions. Nonetheless, the accuracy of the results is a factor of multiple factors, including the accuracy of the input parameters (material properties and boundary conditions), thus necessitating the use of realistic and accurate input parameters to ensure the reliability of the simulations. The performed analysis indicates that the increase in the concrete tensile strength reduces displacements.

**Table 1. Tested slab properties**

| Description | Tested by Lim & Wade [3] |
|---|---|
| Slab thickness, h | 100 mm |
| Length $L_x$ | 4.3 m |
| Width $L_y$ | 3.3 m |
| Support condition | Simply supported |
| Concrete compressive strength, $f_{ck}$ | 36 MPa |
| Concrete aggregates | Siliceous |
| Reinforcing steel yield strength, $f_{yk}$ | 565 MPa |
| Reinforcement | Ø8.7/300mm in both directions |
| Concrete cover | 25 mm |
| Applied Load | 5.4 kN/m$^2$ |

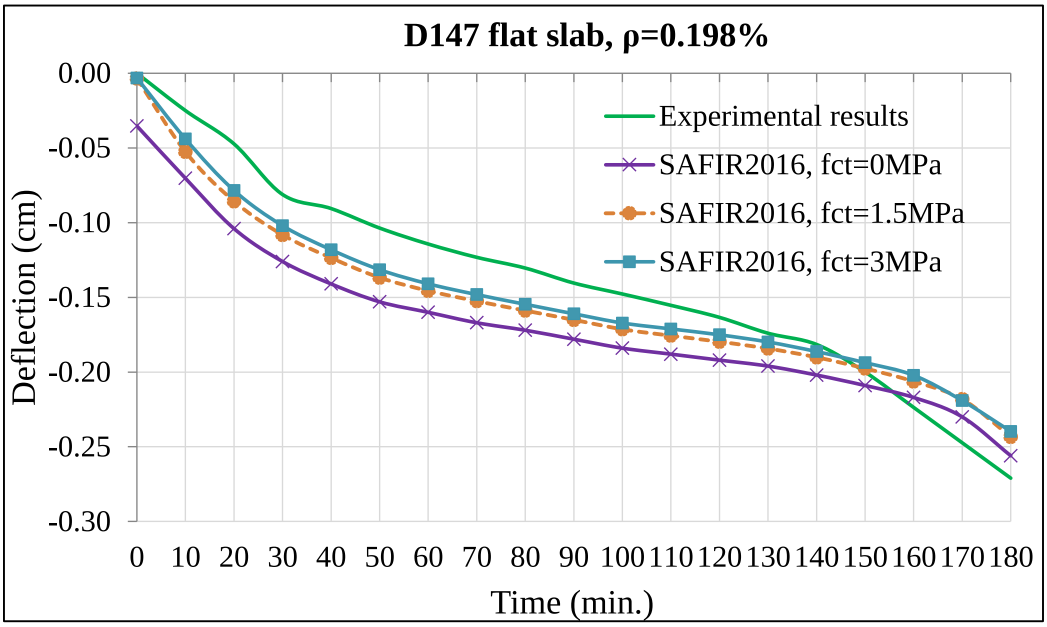


**Figure 7. Comparison of experimentally obtained slab displacements [3] with displacements calculated with SAFIR2016 for different values of concrete tensile strength**

## 5. Results and Discussion

Common properties of the analyzed slabs are shown in Table 2.

**Table 2. Slab properties**

| | |
|---|---|
| Slab thickness, h | 16 cm |
| Concrete compressive strength, $f_{ck}$ | 30 MPa |
| Concrete model | EN 1992-1-2 |
| Concrete aggregates | Siliceous |
| Reinforcing steel yield strength, $f_{yk}$ | 500 MPa |
| Steel model (thermal and mechanical) | Hot rolled (EN 1992-1-2) |
| Dead load (including self-weight), $g_k$ | 5.5 kN/m$^2$ |
| Live load, $q_k$ | 4.0 kN/m$^2$ |
| Design load for normal temperature, $E_d$ | 13.425 kN/m$^2$ |
| Design load in the fire situation, $E_{d,fi}$ [13] | 7.9 kN/m$^2$ |

### 5.1. The Effect of Concrete Cover according to the Simplified Method and Tabulated Data Given in EN 1992-1-2

Table 3 specifies the adopted area of the reinforcement for the design effect of actions for normal temperature design [13]. The slab span is $l_x$=$l_y$=*4 m*.

**Table 3. Main reinforcement area as a function of the different concrete cover thickness ($c_0$)**

| Span (m) | Concrete cover $c_0$=2 cm | | Concrete cover $c_0$=2.5 cm | | Concrete cover $c_0$=3.0 cm | |
|---|---|---|---|---|---|---|
| 4 | Asl,x ($cm^2/m$) | Asl,y ($cm^2/m$) | Asl,x ($cm^2/m$) | Asl,y ($cm^2/m$) | Asl,x ($cm^2/m$) | Asl,y ($cm^2/m$) |
| | 1.65 | 1.65 | 1.72 | 1.72 | 1.80 | 1.80 |

Figure 8 shows the fire resistance of the two-way simply supported slabs exposed to standard fire ISO834. These results were obtained according to the simplified method based on the "Yield Line" theory for slabs and the tabulated data in EN1992-1-2 [1]. The tensile strength of steel is reduced based on the reduction coefficients for the current temperature of the steel found in EN1992-1-2 [1]. The simplified method [1] holds that failure occurs when the maximum bending moment of the slabs approximates the bearing capacity of the slabs due to the action of external loads. High temperatures cause this capacity to decline over time. The bearing capacity of the slabs depends directly on the tensile strength of the reinforcement in the bottom layer, which is exposed to fire and heats up, and loses its strength and stiffness characteristics.

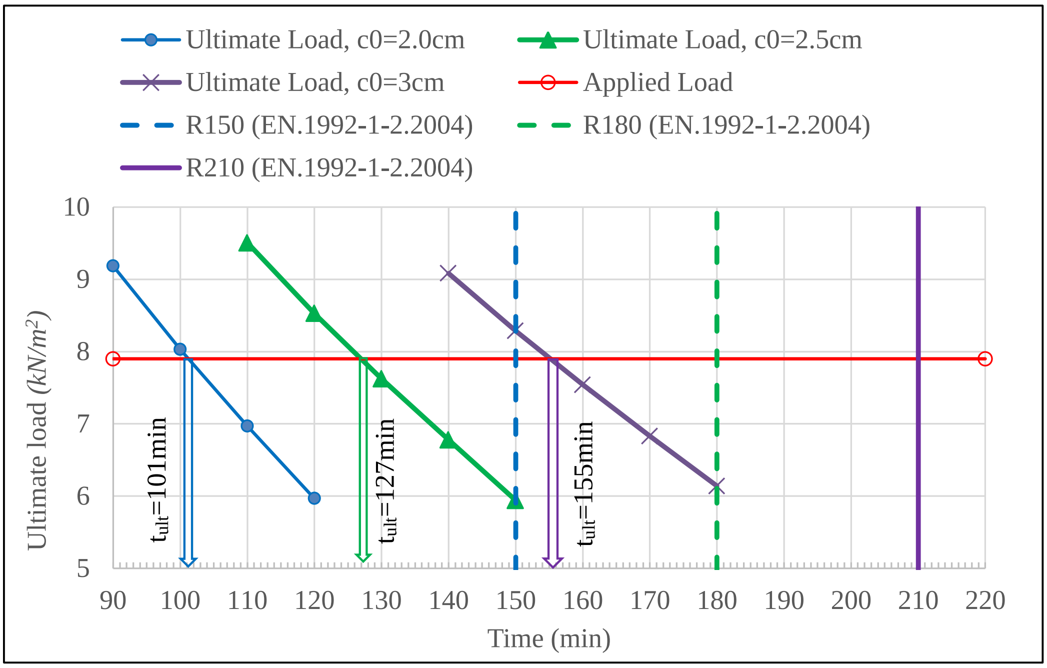


**Figure 8. Fire resistance of two-way simply supported slabs, with span *l=4 m*, according to the simplified method and tabulated data according to EN 1992-1-2.2004, for the concrete cover: $c_0$=2.0 cm, $c_0$=2.5 cm, and $c_0$=3.0 cm**

In EN1992-1-2 [1], the fire resistance of two-way slabs depends mainly on the tensile strength of the steel, which decreases significantly with increasing temperature. Figure 8 and Table 4 show the influence of concrete cover thickness on the fire resistance of slabs: As shown, by increasing the thickness of the concrete cover, the temperature in the reinforcement decreases, leading to a smaller decrease in the tensile strength of the steel and the higher load capacity of the slabs. Figure 8 also demonstrates that concrete cover thickness linearly increases the fire resistance of the slabs. Increasing the concrete cover thickness by 1 cm increases the fire resistance of the slabs by 50%.

**Table 4. Fire resistance of two-way simply supported slabs, with span *l=4 m*, according to the simplified method and tabulated data of EN 1992-1-2.2004, for the concrete cover: $c_0$=2.0 cm, $c_0$=2.5 cm, and $c_0$=3.0 cm**

| Concrete cover $c_0$ (cm) | Axis distance *a* (cm) | Simplified Method (min.) | Tabulated data (min.) |
|---|---|---|---|
| 2.0 | 2.5 | 101 | 150 |
| 2.5 | 3.0 | 127 | 180 |
| 3.0 | 3.5 | 155 | 210 |

Figure 8 and Table 4 suggest there are differences concerning the fire resistance values obtained according to the two methods. The simplified method yielded the smallest values compared to the tabulated data recommended by EN1992-1-2 [1].

The reduction factor of external loads at normal temperature and those in the fire situation according to EN1992-1-2 [1] is.

$$\eta_{fi} = \frac{G_k+\psi_{fi}Q_{k,1}}{\gamma_k G_k+\gamma_{Q,1}Q_{k,1}} = \frac{1.0\times5.5+0.6\times4.0}{1.35\times5.5+1.5\times4.0} = 0.588 \quad (1)$$

For the 2-cm concrete cover and the axial distance of the reinforcement in the first direction *a=2.5 cm*, a fire resistance of 150 minutes is provided according to EN1992-1-2 [1] in tabulated data for two-way slabs. The reduction of the tensile strength of the reinforcement at a distance of *a=2.5 cm* for 150 minutes and steel temperature of $\theta=680°C$ is $k_{s,\theta}=0.278$ according to EN1992-1-2 [1] (Class N for hot rolled reinforcing steel). Since the reduction of tensile strength of the reinforcement is more significant than the reduction of loads for the fire situation (Equation 1) and the area of the adopted reinforcement equals the area of the required reinforcement $A_{sl,prov}=A_{sl,req}$, then, the resistance obtained by apply the simplified method is smaller than that in tabulated data found in EN1992-1-2 [1].

## 5.2. Effect of Concrete Cover according to SAFIR2016 Software

Figure 9 shows the reinforcement schemes of the slabs in the lower and upper layers, as well as the lengths of the reinforcements that are modelled in the numerical calculation in SAFIR2016. Tables 2 and 3 demonstrate the properties of the slabs.

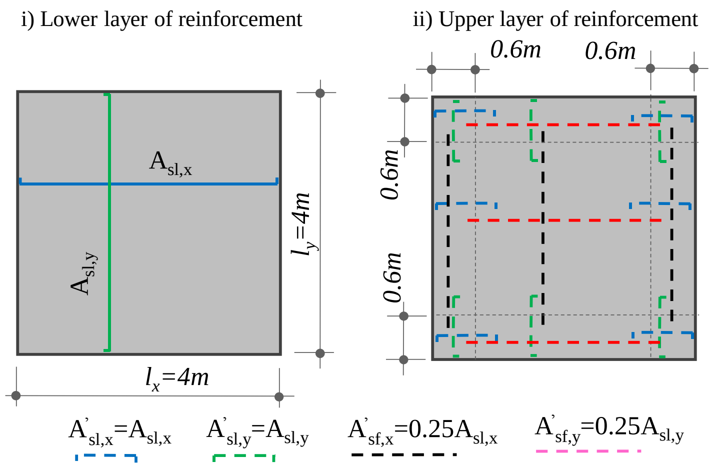


**Figure 9. Reinforcement plan of a simply supported two-way slab**

### 5.2.1. Thermal Response of the Slabs

Figure 10 displays the temperature evolution in slab reinforcement, and Figure 11 illustrates the temperature distribution in the slab exposed to ISO 834 standard fire from the bottom side that was obtained by 3D thermal analysis. The thermal conductivity of concrete is typically much lower than steel. Therefore, concrete provides good thermal insulation to the reinforcement, allowing it to play a pivotal role in the fire resistance of reinforced concrete structures by aiding in limiting the temperature rise of the reinforcement and preventing strength and stiffness loss. For fire durations of one hour and two hours, the temperatures of 868°C and 1016°C are reached on the exposed surface of the slab, respectively, while in the bottom reinforcement, temperatures reach 443°C and 615°C (Figure 10). The top reinforcement's temperature in the slab's unexposed zone gradually increases but remains relatively low, leaving the load-bearing reinforcement capacity intact.

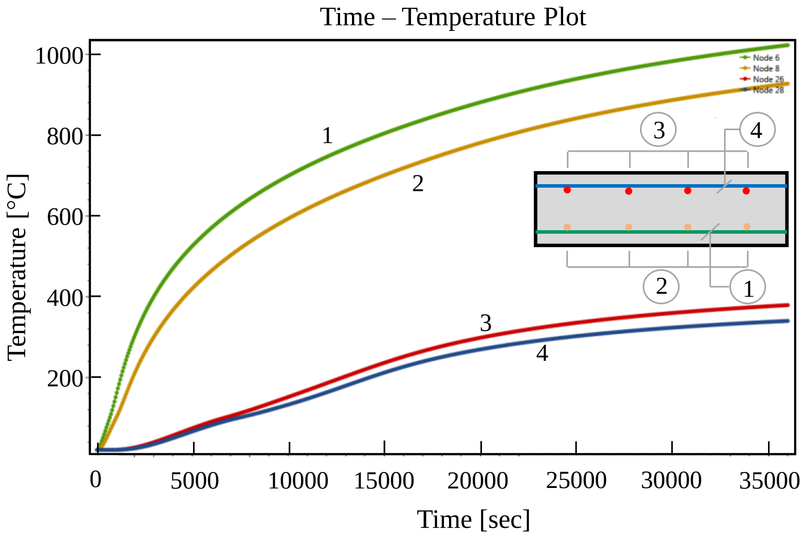


**Figure 100. Temperature evolution in slab reinforcement**

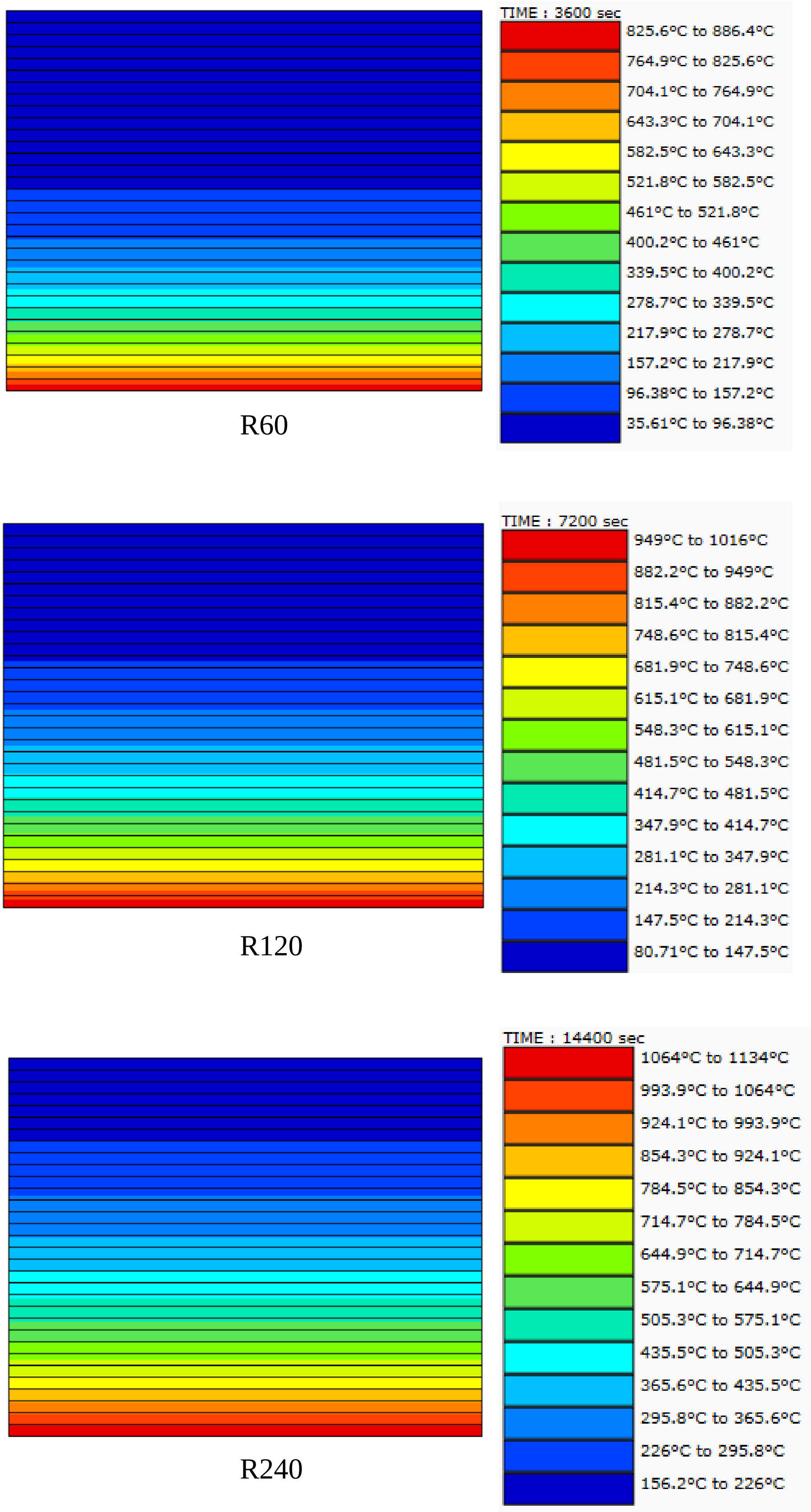


**Figure 11. Temperature distribution in the slab exposed to ISO 834 standard fire, obtained by 3D thermal analysis**

The insulation criteria for fire resistance is typically defined as limiting the temperature rise on the non-exposed surface. For a standard fire, the criterion is often set to an average temperature rise of 140°C over the entire non-exposed surface, with a maximum temperature rise of 180°C at any point on that surface. Assuming the ambient temperature at 20°C, the fire resistance for reinforced concrete slabs with a thickness of 16 cm is achieved after 245 minutes (Figure 12).

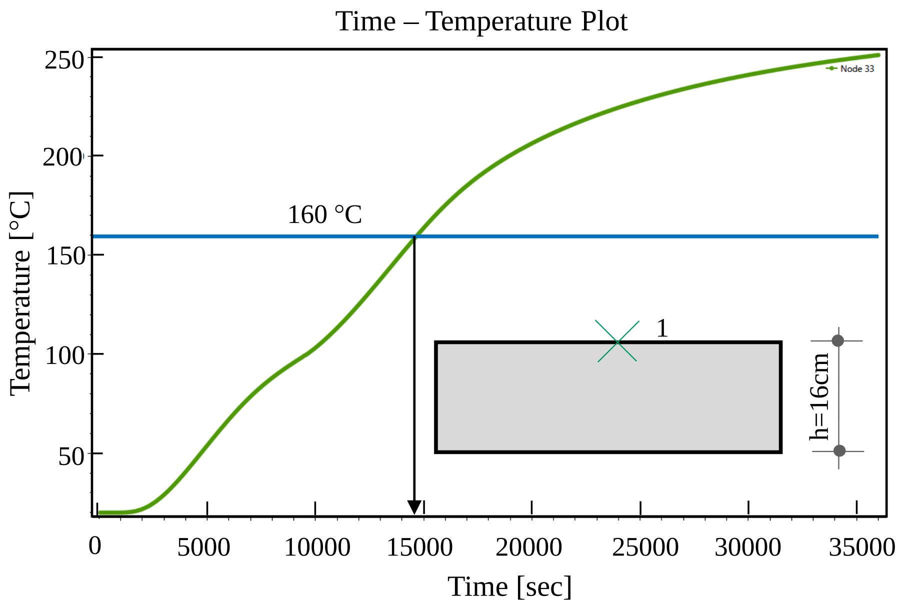


**Figure 11. Fire resistance of the slab according to the insulation criterion**

### 5.2.2. Slab Deflections

Figure 13 shows the maximal vertical displacements of the slab with span $l_x=l_y=4\ m$ (at point D) for different values of the concrete cover thickness when they are exposed to fire from the bottom side. The results are obtained by 3D analysis using SAFIR2016. After ten hours of exposure to fire, the slabs have reached deformations up to *L/10* and have not lost their fire resistance due to the positive impact of membrane forces on the slabs. Figure 13 indicates that the time-displacement curves are broken at specific points. Points (1) occurs when the stresses in the lower reinforcement in the x-x direction, which is closer to the fire-exposed side, reach the steel yield strength for the corresponding temperature. Temperatures in the lower reinforcement in the y-y direction are lower, so after the yield of the reinforcement in the x-x direction, the role of the primary reinforcement in the lower zone is taken over by the reinforcement in the y-y direction. Points (2) occur when reinforcement in the y-y direction reaches the tensile strength of the steel. After this moment, the slab turns into a catenary.

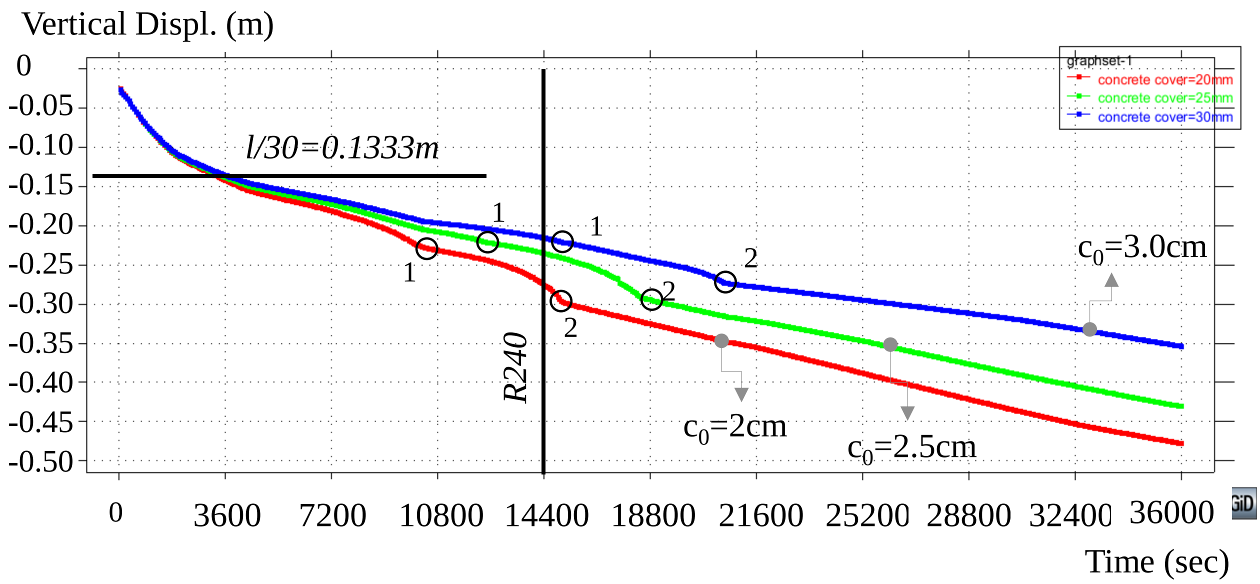


**Figure 12. Influence of the concrete cover thickness on the fire resistance of the simply supported slab with span $l_x=l_y=4m$, according to the 3D analysis with the SAFIR2016**

Table 5 shows the fire resistance of the slabs according to the *L/30* deformation criterion, as well as the deflections of the slabs after four hours of fire exposure. In the case of simply supported slabs, a 1 cm increase in the concrete cover thickness increases the fire resistance by 10%. However, after four hours of fire exposure, the increase of the concrete cover thickness by 1 cm reduces the deflections by 27.9%.

**Table 5. The effect of concrete cover thickness on the deformations of the slabs with span $l_x$=$l_y$=4 m, the time for which the L/30 deflections were reached, as well as the deflections after 4 hours of fire exposure**

| Concrete cover $c_0$ (cm) | 2.0 cm | 2.5 cm | 3.0 cm |
|---|---|---|---|
| Time of L/30 deflections (min.) | 52 | 55 | 57 |
| Deflections after 240 minutes (cm) | 27.5 | 23.5 | 21.5 |

### 5.2.3. Axial Forces and Bending Moments of the Slab

Because of the symmetry of the slab to the two directions, the X-direction and Y-direction, only X-direction axial forces and bending moments are discussed.

Figure 14 shows the main directions of membrane forces in the slabs over time. Along the perimeter of the slabs, ring-shaped compressive membrane forces occur, while tensile membrane forces occur in the span. This mechanism was studied by various researchers in the 1960s and 1970s. It is this mechanism that allows the two-way slab, when the slab loses its bending capacity and plastic hinges appear, to withstand large displacements. The slabs turn into a catenary and can still carry loads.

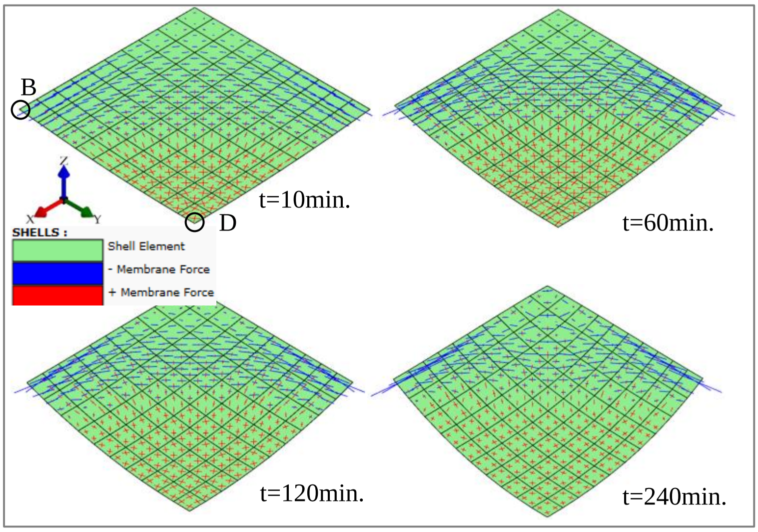


**Figure 13. Main directions of the membrane forces over time**

Figure 15 shows the membrane forces in the x-x direction at point D of the slab. From the diagram, it can be seen that the increase in membrane strength is done gradually until the 50th minute, which corresponds to the plastification of the top reinforcement (point 1). After this moment, the tensile membrane force decreases because the bearing capacity of the slab depends on the hot bottom reinforcement, whose tensile resistance decreases with the increase in temperature. The tensile membrane force is reduced until minute 172 (point 2), where the temperature in the bottom reinforcement is about 700 degrees, and the tensile resistance of the reinforcement drops to 12%. In the 240th minute, the temperature in the lower reinforcement reaches 792 degrees, where the reduction in the tensile strength of the reinforcement is 11%.

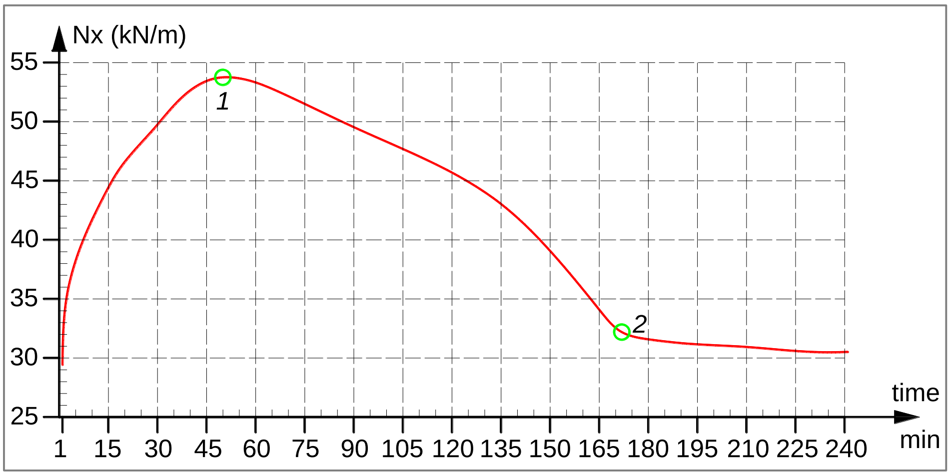


**Figure 14. Nx tensile forces over time at point D**

Knowing that after 120 minutes, the entire force is accepted by the reinforcement, as well as knowing the area of the top and bottom reinforcement (Table 3), the current temperature in the reinforcement, and the coefficient of reduction of tensile strength in the reinforcement, then we can verify the value of obtained the tensile strength of the membrane at the time 172 minutes from the numerical analysis done by SAFIR2016.

$$N_{x,172} = A_{slx,bottom} \times f_{sd,fi} + A_{slx,top} \times f_{sd,cold} = 165 \times 0.12 \times 500 + 45 \times 500 = 32400N = 32.4\ kN \quad (2)$$

Figure 16 shows the membrane forces in the x-x direction in the strip b-d over time. In the initial phase, there are small membrane forces in tension in the midspan as well as small membrane forces in compression in the peripheral part of the slab. In this phase, the loads are resisted by bending (Figure 17). After 30 minutes, pronounced tensile membrane forces in the *1.5m* strip width and compressive membrane forces in the *0.5m* strip width are presented. From the 30th minute, the slab resisted the vertical load only through the membrane forces, while the bending moments reached 0 (Figure 17).

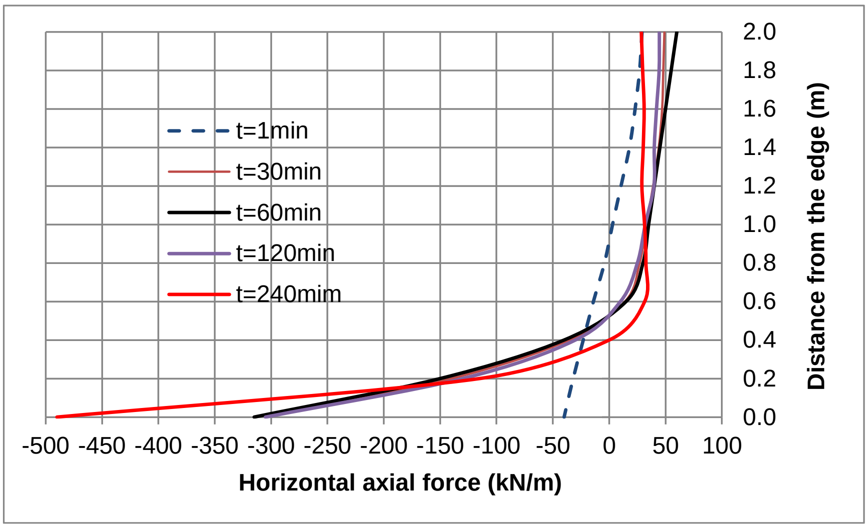


**Figure 15. Nx forces at strip B-D over time**

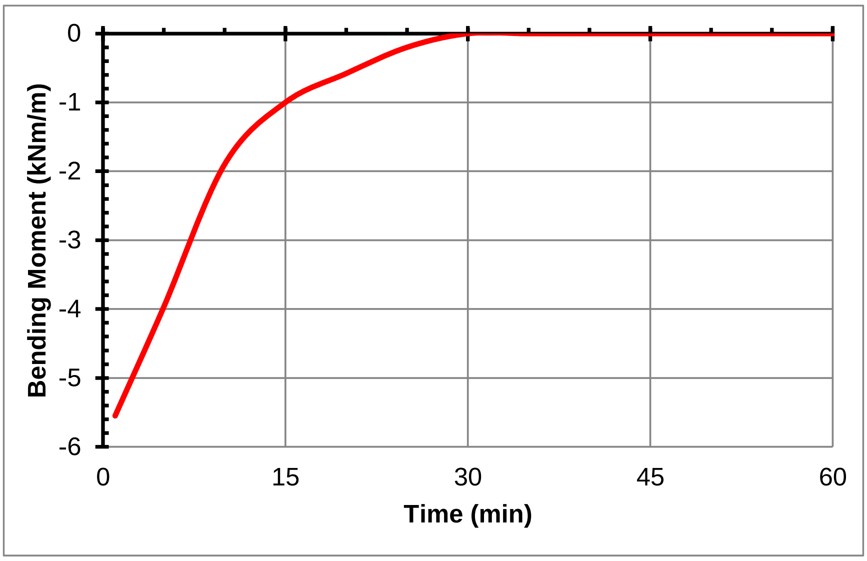


**Figure 16. Slab bending moments about X-axis over time at point D**

### 5.2.4. Concrete and Reinforcement Stresses

With the symmetry of the slab to the two directions – the X and Y directions – only the X-direction axial concrete and reinforcement stresses are discussed.

Figure 18 shows the concrete compressive stresses in the x-x direction over time on the section at point D, obtained by numerical analysis through the SAFIR2016 software. The compressive stresses in the slab are affected by both the action of vertical loads and the fire from the bottom side. The vertical loads cause bending in the slab, leading to compressive stresses in the upper fibers. Meanwhile, the fire causes nonlinear temperature and thermal expansions change, leading to thermal stresses in the slab. The fulfilments of Bernoulli's hypothesis is a prerequisite for slabs with a high span-to-depth ratio, suggesting that that plane cross sections must remain plane. This forms compressive stresses in the bottom fibers from mechanical dilatations. The stresses from the temperature change are more pronounced in the first 30 minutes of the fire when the stiffness of the element is greater. As the fire continues, the slab experiences membrane forces in traction in the span and compression in the perimeter, which eventually leads to the slab working entirely in tension after 120 minutes. At this point, the compressive stresses in the concrete are equal to zero, and the entire load is accepted by the reinforcement. The slab becomes catenary in shape, with the reinforcement providing the necessary support Figure 19.

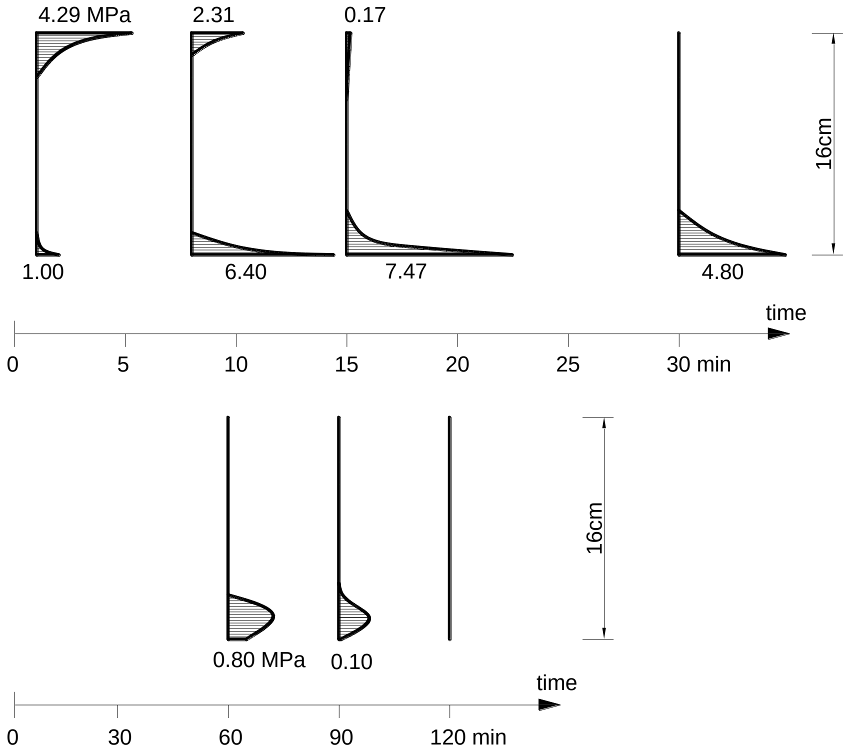


**Figure 17. Concrete compressive x-x stresses over time at point D**

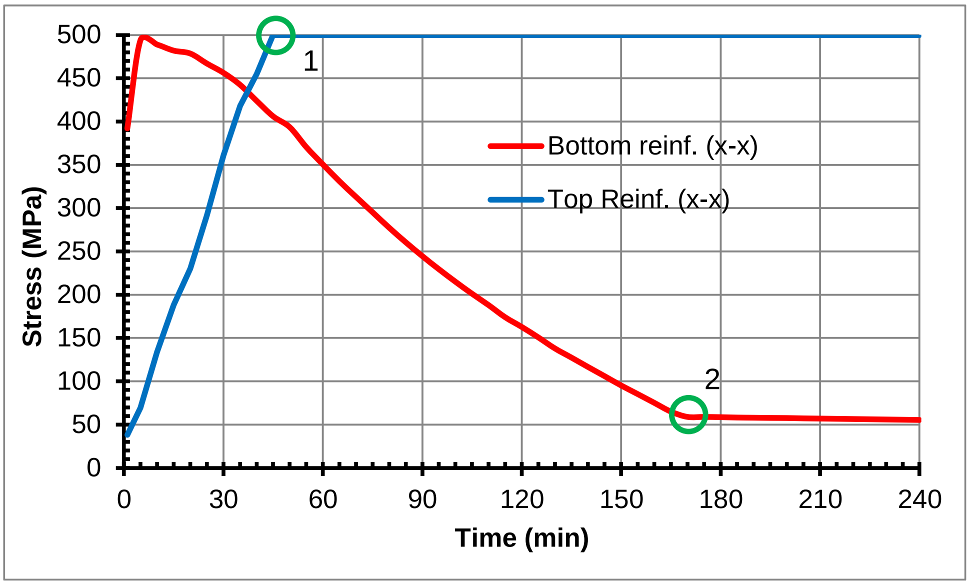


**Figure 18. Stresses in x-x reinforcement over time at point D**

Figure 19 shows the tensile reinforcement stresses in the x-x direction over time on the section at point D, obtained by numerical analysis. For the cold upper reinforcement, a typical "$\sigma - \varepsilon$" diagram is obtained for steel at ambient temperature, while for the heated lower reinforcement, an apparent stress drop occurs, which is the result of the reduction in the tensile strength of the steel. If the values are expressed as a percentage of the current load capacity of the steel, it will be noted that they are close to the yield strength of the steel Figure 20.

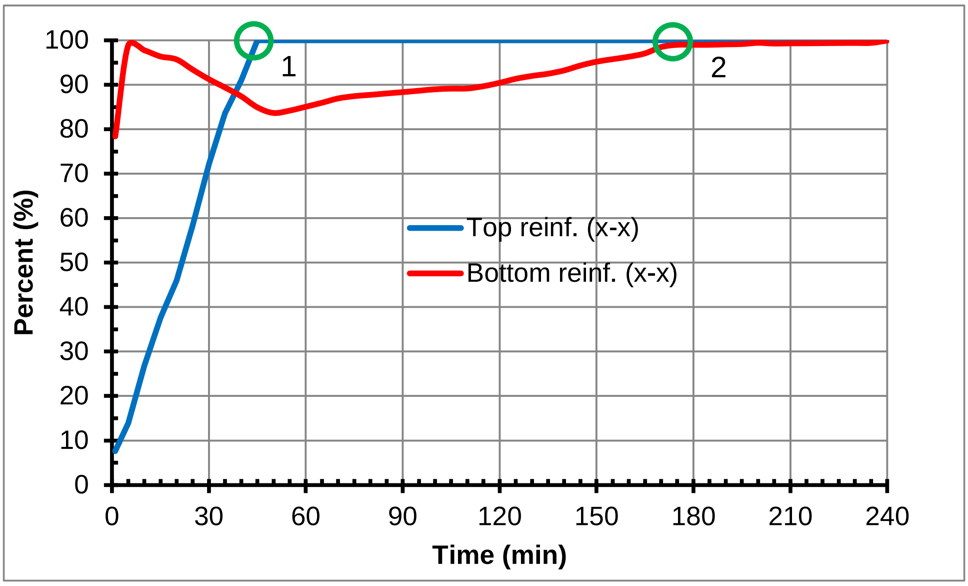


**Figure 19. Stresses in x-x reinforcement over time at point D expressed as a % of the current value of the yield strength of the steel**

The top reinforcement, although secondary, increases the fire resistance of slabs if placed along the entire slab span. The better behavior of the slabs can be related to the activation of the top secondary reinforcement to resist the membrane forces:when the vertical displacements are extremely large, and the slab works like a catenary.

### 5.3. Comparison of Fire Resistance to Two-Way Slabs according to SAFIR2016, the Simplified Method, and Tabulated Data Given in EN 1992-1-2

Table 6 compares the fire resistance values of slabs obtained according to SAFIR2016, the simplified method, and tabulated data given in EN1992-1-2 [1]. This software provides more accurate results by considering additional factors, such as tensile membrane forces (Figure 14 and Figure 16), to increase the fire resistance of two-way slabs. Nonetheless, the simplified method and tabulated data provided in EN1992-1-2 [1] are still useful for initial design and quick assessments, as they are more conservative and on the safe side. It is recommended to use the 3D analysis for more detailed and accurate assessments, especially for critical structures.

**Table 6. Fire resistance of two-way simply supported slabs, with span $l_x=l_y=4m$, according to SAFIR2016, simplified method and tabulated data according to EN 1992-1-2.2004, for the concrete cover: $c_0=2.0$ cm, $c_0=2.5$ cm, and $c_0=3.0$ cm**

| Concrete cover $c_0$ (cm) | Axis distance *a* (cm) | Simplified Method (min.) | Tabulated data (min.) | SAFIR2016 (min.) |
|---|---|---|---|---|
| 2.0 | 2.5 | 101 | 150 | >600 |
| 2.5 | 3.0 | 127 | 180 | >600 |
| 3.0 | 3.5 | 155 | 210 | >600 |

### 5.4. Effect of Slab Span according to SAFIR2016

Table 7 specifies the adopted area of the reinforcement for the design effect of actions for normal temperature design.

**Table 7. Main reinforcement area as a function of the different slab span ($l_x=l_y$)**

| Span $l_x=l_y$ (m) | Concrete cover thickness $c_0$=2cm | |
|---|---|---|
| | $A_{sl,x}$ ($cm^2$/m) | $A_{sl,y}$ ($cm^2$/m) |
| 4 | 1.65 | 1.65 |
| 5 | 2.50 | 2.50 |
| 6 | 3.78 | 3.78 |

Figure 21 shows the vertical displacements (at point D) of two-way slabs with different spans and a concrete cover of *2cm*. Figure 21 indicates that with the increase of span, the vertical displacements also increase; therefore, according to the criterion of acceptable displacements L*/30*, the fire resistance decreases although insignificantly since with the increase of the slab span, the value of the allowed deformations increases. Figure 21 and Table 8 indicate that according to the criterion of allowed deformations L/30, with the increase of the slab span by one meter, the fire resistance decreases by 6%. After four hours of fire action, from the obtained results, it can be seen that the maximum deformations in the slabs have a value of about L/15. After ten hours of exposure to fire, the slabs reached deformations up to *L/10* and maintained their fire resistance due to the positive impact of membrane forces on the slabs.

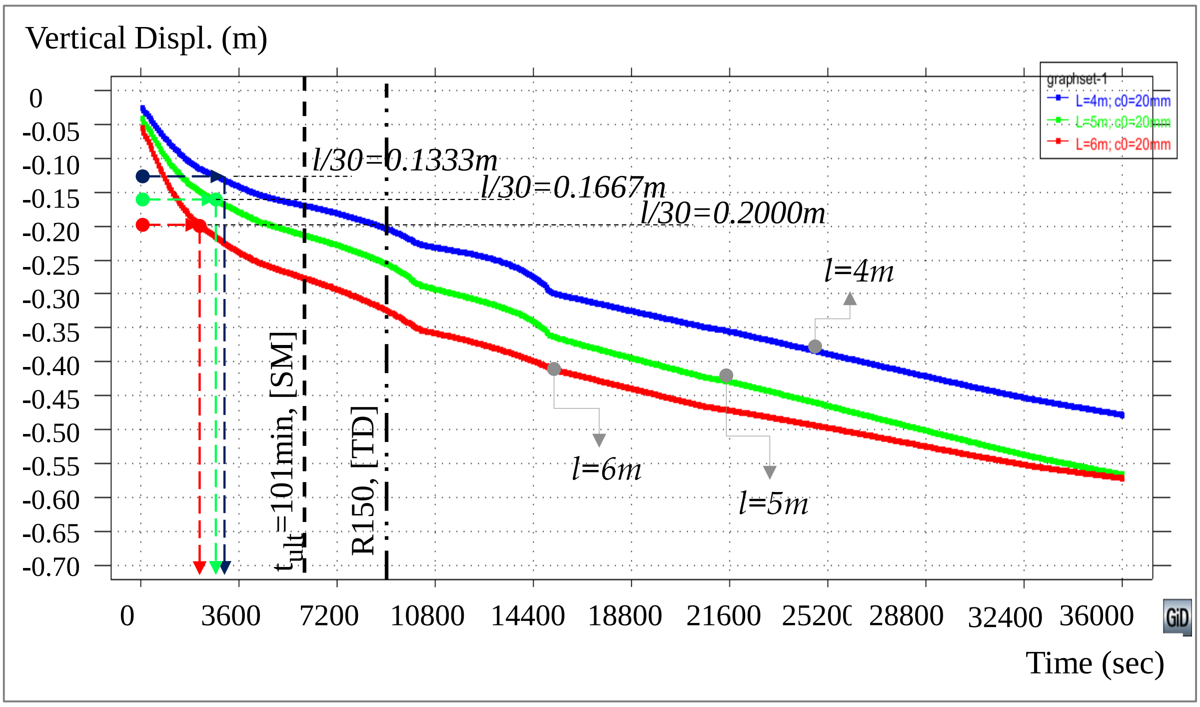


**Figure 20. Influence of the slab span on fire resistance of simply supported slab according to 3D analysis with SAFIR2016 and according to the simplified method and tabulated data**

**Table 8. The effect of slab span on the deformations, the time for which the L/30 deformations were reached, as well as the deformations for the time t=240 minutes**

| **Span $l_x$=$l_y$ (m)** | **4** | **5** | **6** |
|---|---|---|---|
| Time of L/30 deflections (min.) | 52 | 49 | 47 |
| Deflections after 240 minutes (cm) | 27.5 | 34 | 40 |

According to the ultimate state criterion, all the slabs showed resisted fire for over ten hours. According to the simplified method, they lost resistance at the same time because the initial stresses in the reinforcement for all the slabs were the same, as well as the reduction in the tensile strength of the reinforcement for the same concrete cover. Also, according to the tabulated data, the slabs with different spans display equal fire resistance because the concrete cover is equal for all three cases.

## 5.5. Effect of the Effect of Support Conditions on the Fire Resistance of Two-Way Slabs

Figure 22 shows the support conditions for two-way slabs with span $l_x$=$l_y$=*5* m and concrete cover $c_0$=*2.0* cm, analyzed using SAFIR2016. The provided area of the primary reinforcement in the top and bottom zone for all slabs is equal to the required reinforcement (Table 9). The length of the main top reinforcement has been adopted according to the recommendations given in EN1992-1-2 [1]. The anchorage length must be added to the reinforcement length of the top zone, as shown in Figure 22.

**Table 9. Main reinforcement area as a function of support conditions**

| **Reinforcement Area (cm$^2$/m)** | **Slab** | | | | | |
|---|---|---|---|---|---|---|
| | **S1** | **S2** | **S3** | **S4** | **S5** | **S6** |
| Span $A_{sl,x}$ | 2.59 | 2.30 | 1.87 | 1.80 | 1.57 | 1.25 |
| Span $A_{sl,y}$ | 2.59 | 1.90 | 1.25 | 1.80 | 1.31 | 1.25 |
| Support $A_{sl',x}$ | | 3.75 | 3.00 | 3.00 | 2.57 | 2.15 |
| Support $A_{sl',y}$ | | | | 3.00 | 2.28 | 2.15 |

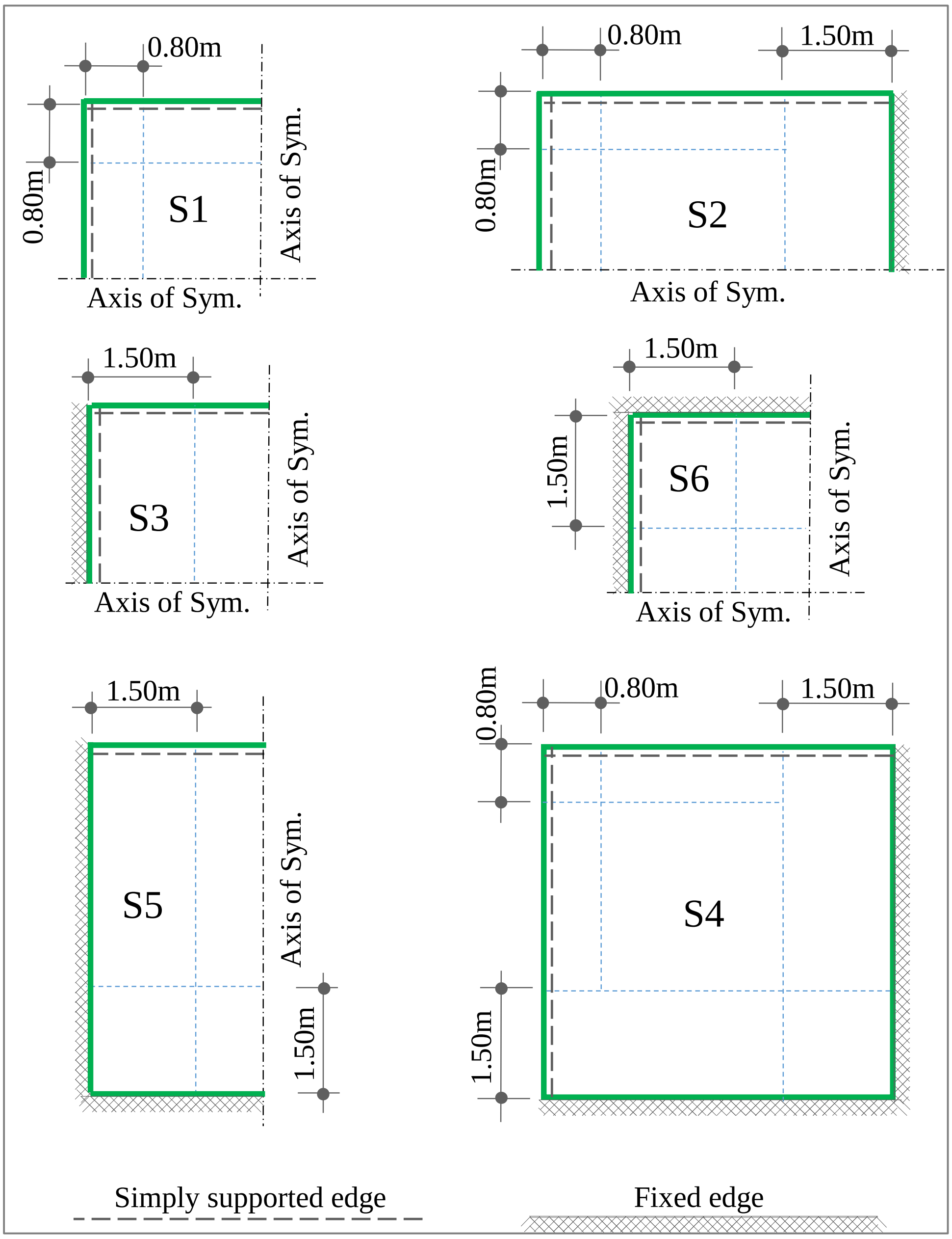


**Figure 21. Support conditions of analyzed two-way slabs with span $l_x$=$l_y$=5m and concrete cover $c_0$=2.0 cm**

Note that the anchorage length is necessary to ensure that the reinforcement can develop its full strength and transfer the loads to the concrete. The length of the anchorage is dependent on several factors, such as the diameter of the reinforcement, the strength of the concrete, and the bond strength between the reinforcement and the concrete [14-18]. The design of the anchorage length should follow the guidelines given in the relevant design code, such as [1, 12], to ensure the safe and efficient transfer of loads between the reinforcement and the concrete.

Figure 23 shows the maximal vertical displacements of the slabs with various support conditions. All slabs have a span of $l_x$=$l_y$=5 *m* and a concrete cover thickness of $c_0$=2 *cm*. In terms of bearing capacity, all slabs showed fire resistance of higher than ten *hours*. Table 10 shows that in terms of deflections, the supporting conditions of the slabs have a significant influence on their behavior. The slab with simply supported edges (S1) has the highest deflection under fire conditions, while the slab with fixed edges (S6) has the lowest deflection since fixed edges prevent slab rotation and thus increase stiffness and decrease deflection under fire conditions. The time to reach L/30 displacements in the slab fixed on four edges (S6) is almost three times greater compared to the slab simply supported on four edges (S1). Also, the deflections of the slabs after 4 hours, which is the maximum time required for fire resistance of these elements according to fire safety regulations, in the case of the S6 slab, are about 60% smaller than in the case of the S1 slab. The slab with one edge simply supported and one fixed edge has intermediate deflection between the two extreme cases. This is because the fixed edge still provides some resistance to rotation, but not as much as two fixed edges. It is important to consider the effects of support conditions on slab behavior under fire conditions, as it can significantly affect the overall performance of the structure.

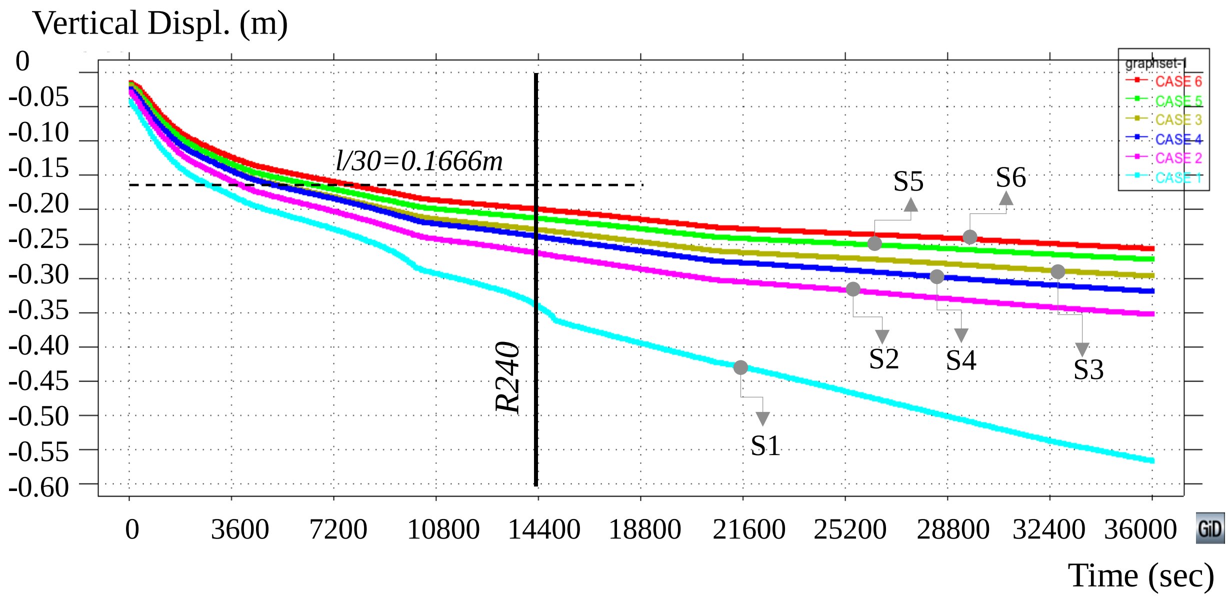


**Figure 22. Vertical displacements in two-way slabs for different support conditions and fire from the bottom side**

**Table 10. Main reinforcement area as a function of support conditions**

| Slab | S1 | S2 | S3 | S4 | S5 | S6 |
|---|---|---|---|---|---|---|
| Time of L/30 deflections (min.) | 49 | 67 | 92 | 89 | 113 | 136 |
| Deflections after 240 minutes (cm) | 34.0 | 26.4 | 22.9 | 24.0 | 21.3 | 20.0 |

## 6. Conclusions

Below are the conclusions drawn from this study. The application of these conclusions to the design of reinforced concrete slabs can significantly increase the fire safety of buildings.

- In two-way, simply supported slabs exposed to fire from the bottom side, by increasing the span, the vertical displacements increase. This is while, according to the load-bearing criteria, the two-way slabs have high fire resistance, much higher than the permissible level mentioned in the fire safety regulations. The high load-bearing capacity in fire conditions can be attributed to the initiated membrane tensile forces that are more pronounced at larger vertical displacements. According to the criterion of allowed deformations L/30, with the increase of the slab span by one meter, the fire resistance decreases by 6%. After four hours of fire action, the maximum deformations in the slabs reached L/15.
- Increasing the concrete cover thickness in two-way, simply supported slabs can indeed improve their fire resistance by providing additional protection to the reinforcing steel against high temperatures during the fire. The concrete cover acts as a thermal insulator, slowing down the transfer of heat from the fire to the reinforcement. According to the L/30 deflection criterion, increasing the concrete cover thickness by 1 cm increases the fire resistance by 10%. After 4 hours of fire exposure, the increase in the concrete cover thickness of 1 cm reduces the deflections by 27.9%. However, this increase in fire resistance is limited, and the excessive increase in the concrete cover thickness may not be practical. Therefore, while increasing the concrete cover thickness can improve the fire resistance of two-way slabs, it should be done within practical limits by following structural, construction, and durability considerations.
- If two-way slabs are analyzed according to the simplified method based on the Yield Line Theory of slabs, the concrete cover thickness linearly increases the fire resistance of the slab. According to this method, increasing the concrete cover thickness by 1 cm increases the fire resistance of the slabs by 50%. The span does not affect the fire resistance because the simplified method does not include the influence of membrane tensile forces, which are more pronounced at larger vertical displacements and increase the load-bearing capacity of the slab.
- Two-way slabs exposed to fire from the bottom side have better fire performance when they are fixed on all four sides. This is because reducing the number of fixed sides increases the vertical displacements in the span and decreases the fire resistance in terms of deflections. If the slab is fixed on two sides, better behavior is achieved when the fixation is on two opposite sides than on two adjacent sides. The time to reach L/30 displacements in the slab fixed on four edges is almost three times greater than the case in which the slab is simply supported on four edges. The deflections of the slabs after four hours, which is the maximum time required for fire resistance of these elements according to fire safety regulations, in the case of the slab fixed on all four sides, are about 60% smaller than in the case of the simply supported slab.

- The top reinforcement, although secondary, if placed along the entire slab span, increases the fire resistance of slabs. The reason for the better behavior of the slabs is the activation of the top secondary reinforcement to resist the membrane forces, when the vertical displacements are extremely large, and the slab works like a catenary.
- The fire safety regulations usually prescribe conservative values for the fire resistance of structural elements, which may lead to overdesign and unnecessary costs. Therefore, it is recommended to perform a detailed analysis of the behavior of reinforced concrete two-way slabs in fire conditions to optimize the design and increase the fire safety of the building.

## 7. Declarations

### 7.1. Author Contributions

Conceptualization, F.S., Z.G., M.C., and F.P.; methodology, F.S., Z.G., and M.C.; software, F.S., Z.G., and M.C.; validation, F.S., Z.G., and M.C.; formal analysis, F.S., Z.G., M.C., and F.P.; investigation, F.S., Z.G., and M.C.; resources, F.S., Z.G., and M.C.; data curation, F.S. and Z.G.; writing—original draft preparation, F.S. and M.C.; writing—review and editing, F.S., Z.G., M.C., and F.P.; visualization, F.S. and Z.G.; supervision, M.C. and F.P.; project administration, F.S., Z.G., and F.P.; funding acquisition, F.S., Z.G., M.C., and F.P. All authors have read and agreed to the published version of the manuscript.

### 7.2. Data Availability Statement

The data presented in this study are available in the article.

### 7.3. Funding

The authors received no financial support for the research, authorship, and/or publication of this article.

### 7.4. Conflicts of Interest

The authors declare no conflict of interest.

## 8. References

[1] EN 1992-1-2. (2004). Eurocode 2: Design of concrete structures - Part 1-2: General rules - Structural fire design. European Committee for Standardization (CEN), Brussels, Belgium.

[2] Moss, P. J., & Charles Clifton, G. (2004). Modelling of the Cardington LBTF steel frame building fire tests. Fire and Materials, 28(24), 177–198. doi:10.1002/fam.868.

[3] Lim, L. C. S., & Wade, C. A. (2002). Experimental fire tests of two-way concrete slabs. Fire Engineering Research Report 02/12, University of Canterbury, Christchurch, New Zealand

[4] Bailey, C. G., & Toh, W. S. (2007). Behaviour of concrete floor slabs at ambient and elevated temperatures. Fire Safety Journal, 42(6–7), 425–436. doi:10.1016/j.firesaf.2006.11.009.

[5] Jiang, J., & Li, G. Q. (2018). Parameters affecting tensile membrane action of reinforced concrete floors subjected to elevated temperatures. Fire Safety Journal, 96, 59–73. doi:10.1016/j.firesaf.2017.12.006.

[6] Wang, Y., Dong, Y. L., & Zhou, G. C. (2013). Nonlinear numerical modeling of two-way reinforced concrete slabs subjected to fire. Computers and Structures, 119, 23–36. doi:10.1016/j.compstruc.2012.12.029.

[7] Liao, F., & Huang, Z. (2015). An extended finite element model for modelling localized fracture of reinforced concrete beams in fire. Computers and Structures, 152, 11–26. doi:10.1016/j.compstruc.2015.02.006.

[8] Abu, A. K., Burgess, I. W., & Plank, R. J. (2013). Tensile Membrane Action of Thin Slabs Exposed to Thermal Gradients. Journal of Engineering Mechanics, 139(11), 1497–1507. doi:10.1061/(asce)em.1943-7889.0000597.

[9] Buchanan, A. H., & Abu, A. K. (2016). Structural Design for Fire Safety. Wiley, Hoboken, United States. doi:10.1002/9781118700402.

[10] Johansen, K. W. (1968). Yield-line formulae for slabs. CRC Press, Boca Raton, United States. doi:10.4324/9780203221853.

[11] Franssen, J. M., & Gernay, T. (2016). User's manual for SAFIR 2016c A computer program for analysis of structures subjected to fire. University of Liege, Liège, Belgium.

[12] EN 1992-1-1. (2004). Eurocode 2: Design of concrete structures - Part 1-1: General rules and rules for buildings. European Committee for Standardization (CEN), Brussels, Belgium.

[13] EN 1991-1-2. (2002). Eurocode 1: Actions on structures - Part 1-2: General actions - Actions on structures exposed to fire. European Committee for Standardization (CEN), Brussels, Belgium.

[14] Shakiba, M., Oskouei, A. V., Karamloo, M., & Doostmohamadi, A. (2021). Effect of mat anchorage on flexural bonding strength between concrete and sand coated GFRP bars. Composite Structures, 273, 114339. doi:10.1016/j.compstruct.2021.114339.

[15] Mak, M. W. T., & Lees, J. M. (2022). Bond strength and confinement in reinforced concrete. Construction and Building Materials, 355, 129012. doi:10.1016/j.conbuildmat.2022.129012.

[16] Krishnaveni, S., & Rajendran, S. (2022). A state of the art on characterization and application of artificial neural networks on bond strength between steel rebar and concrete. Construction and Building Materials, 354, 129124. doi:10.1016/j.conbuildmat.2022.129124.

[17] Ahmed, K. S., Shahjalal, M., Siddique, T. A., & Keng, A. K. (2021). Bond strength of post-installed high strength deformed rebar in concrete. Case Studies in Construction Materials, 15, e00581. doi:10.1016/j.cscm.2021.e00581

[18] Li, Z., Qi, J., Hu, Y., & Wang, J. (2022). Estimation of bond strength between UHPC and reinforcing bars using machine learning approaches. Engineering Structures, 262, 114311. doi:10.1016/j.engstruct.2022.114311.